

2 Diffractometers and Reflectometers

In the previous chapter we described the basic elements of x-ray equipment, namely, x-ray sources, optical elements to define the beam pass and a proper band pass of energy, and various recording units to detect the x-rays. In this chapter we deal with the experimental arrangement as a whole. There are general aspects to consider in setting-up an x-ray experiment: The sample is illuminated by an incident beam striking the sample surface under a definite angle of incidence α_i . The incident beam may be characterized by its incident divergence $\Delta\alpha_i$ and its energy spread $\Delta\lambda$. After interaction of the beam with the sample, the scattering intensity escaping from the surface at a take-off angle α_f has to be recorded. Owing to the finite size of the detector window, all the photons leaving the sample surface in a take-off angle range $(\alpha_f - \Delta\alpha_f/2, \alpha_f + \Delta\alpha_f/2)$ are registered by the detector simultaneously. The plane containing the source and the surface normal of the sample is called the *scattering plane*. Since the scattering happens within the scattering plane, the scattering geometry is called *coplanar*. In the so-called *not coplanar* or *off-plane* scattering geometry (Sect. 4.3), the directions of the incident and the scattered beams are also characterized by the azimuthal angles θ_i and θ_f and by the widths of the corresponding angular intervals $\Delta\theta_i$ and $\Delta\theta_f$.

Different problems of measurement require slightly different diffractometer arrangements. X-ray reflectometry uses scans at very small α_i . If one is interested in thin-film analysis, high-resolution in angular space is not necessary. As shown later, a β -filtering of the white spectrum of an x-ray tube gives sufficient energy resolution so long as the layer thickness to be analyzed does not approach the micron range and so long as one is not interested in recording reciprocal-space maps.

The situation is different for wide-angle diffractometry. Here high resolution in energy and angular space is necessary for analyzing the lattice misfit between epilayer and substrate even for nearly lattice-matched heterostructures. High resolution also guarantees the low noise also necessary for analyzing very thin films. High resolution is obtained by using optical elements. As shown in Section 1.2 these elements reduce $\Delta\alpha_i$ and/or $\Delta\alpha_f$ at the cost of decreasing the integrated scattering power. This has to be compensated for by insertion of photon collectors as beam compressors or Göbel mirrors or otherwise by increasing the recording time per angular step. Often

one has to compromise between the degree of resolution and the time necessary for measurement. In this chapter we will show that high resolution is not required in general. Samples with mosaic spread, heterostructures with a large lattice mismatch or epilayers with a thickness of a few 100 nm can be investigated under slightly relaxed conditions of resolution without loss of information.

2.1 X-Ray Reflectometers

X-ray specular reflectometry is used to measure the thickness of individual thin layers, the vertical spacing of a multilayer stacking, the surface and interface roughnesses, and the average density of a layered system. According to the α_i^{-4} law of Fresnel reflectivity (Sects. 5.2 and 6.4), the intensity leaving a smooth surface decreases very rapidly as the angle of incidence increases. To record the reflected intensity over more than 6 orders of magnitude one needs a highly intensive incident beam and/or a detector with low noise.

The apparative requirements should be demonstrated by the following examples. In case of layered samples the layer thickness is determined from the angular distance between the thickness oscillations (Kiessig maxima, see Sect. 8.1). The required angular resolution depends on the total thickness of film. Film thicknesses of about 50 nm provide an angular distance between Kiessig maxima of about 0.1° . Such a film can be investigated using the $\text{CuK}\alpha$ -doublet of a sealed tube collimated by two spatially separated located slits before the sample and and an additional slit placed before the detector.

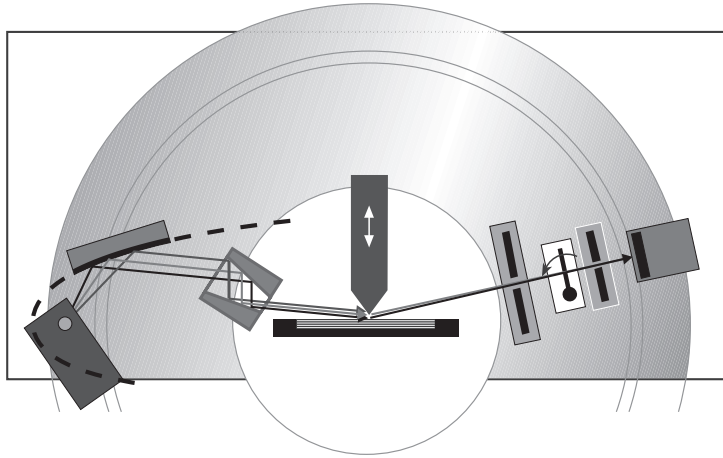


Fig. 2.1. General setup of a high-resolution x-ray reflectometer.

The precise determination of the critical angle of total external reflection, α_c , which is necessary for electron density analysis, demands a much better angular resolution. Often it is sufficient to match α_c approximately with the angular position of half-intensity compared with the primary beam (Sect. 8.1). The average density is obtained with an accuracy of 5% if α_c is measured to an accuracy of 2.3%. It requires precise angle adjustment on the order of 0.001° .

It follows from these previous estimates that a reflectivity experiment needs high flux at the sample site, moderate angular resolution in most cases, but accurate angle adjustment between sample and detector circle. At home-laboratories an angle-dispersive reflectometer (Fig. 2.1) should consist of the source attached to a photon-collecting system as Göbel-mirror (completed by beam compressor), horizontal and vertical slits to define the beam size, and a detector with a large dynamical range. The slits can be inserted either before or after the sample. The angular resolution of the experiment is additionally controlled by a knife-edge attached close to the center of goniometer. Both the sample circle, denoted by ω , and the detector circle, 2θ , move with an accuracy of $\Delta\omega = \Delta 2\theta \leq 0.001^\circ$.

The specular reflectivity is recorded by running an $\omega/2\theta$ scan, where ω corresponds to the true angle of incidence α_i and 2θ is the angular position of the detector measured with respect to the incident beam direction. Both α_i and the exit angle $\alpha_f = 2\theta - \alpha_i$ are moving simultaneously by the same amount. With so-called θ - θ reflectometers, where the sample stays fixed, α_i and α_f vary directly instead of $\omega = \alpha_i$ and $2\theta = \alpha_i + \alpha_f$ which is the case with at equipment, where the x-ray tube is fixed. The properties of the $\omega/2\theta$ scan and others with different angular ratios will be described in Sect. 3.2 in detail.

The function of the knife-edge, shown in Fig. 2.1, can be explained as follows. For geometrical and intensity reasons, both $\Delta\alpha_i$ and $\Delta\alpha_f$ cannot be reduced too much. Because the incident beam divergence and the detector acceptance are large, the irradiated sample area must be reduced to achieve sufficient angular resolution. This is achieved by sinking the knife-edge very close to the axis of goniometer rotation, which additionally helps to bring the sample surface to the rotation center (see below). Under these conditions, only those parts of the beam reach the detector, which are escaping the sample straight beneath the knife-edge. The extreme limitation of the scattering area reduces the detectable intensity by several orders of magnitude. This disadvantage can be compensated for by insertion of a photon collector in front of the sample (see Fig 1.9).

An alternative setup is shown in Fig. 2.2. The first Göbel-mirror is sufficient to suppress the $K\beta$ line. High resolution still can be achieved by replacing the beam compressor in Fig. 2.1 by a Bartels monochromator (Sect. 1.2 and Fig. 1.8). Relaxed resolution but higher flux is achieved by removing the beam compressor but setting a second Göbel mirror in front of the

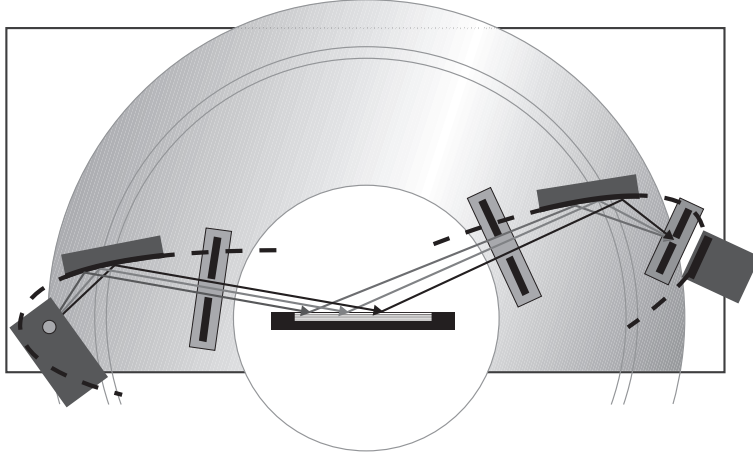


Fig. 2.2. Scheme of a powder diffractometer applied for x-ray reflectometry with relaxed angular resolution.

detector. The gain of detected intensity is due to the fact that the second Göbel mirror increases the beam cross section. Specularly and non-specularly scattering photons are deflected toward the center of a point detector. This set-up corresponds to that of a powder diffractometer [167].

At synchrotron facilities the incident beam is parallel enough. The reflectometer has to be equipped vertically in order to make use of the extreme collimation of the incident beam in this direction (see Sect 1.1). For angular dispersive experiments one has to insert an optical element for monochromizing the incident x-ray spectrum. This can be done either before or after the sample.

A completely different arrangement is necessary to perform an energy-dispersive experiment (Fig. 2.3) [57]. Here the white beam strikes the sample surface under a fixed $\omega = \alpha_i$ and the reflected beam is recorded by an energy-dispersive detector at a fixed angle $2\theta = \alpha_i + \alpha_f$. In this case the only requirement is an approximately parallel incident beam provided at a synchrotron facility without optical elements except slits. In a home laboratory a sufficiently parallel beam is prepared by passing the beam through two slits fixed at both ends of an about 1-meter-long tube, which should be evacuated to reduce air scattering and absorption by air. Only low air absorbance supplies the whole white spectrum of an x-ray tube [238]. The resolution of an energy-dispersive scattering experiment is determined by the energy resolution of the detector. It amounts to $(\Delta E/E \leq 2.5\%)$, which is sufficient for thin film analysis. The advantage of this set-up is the possibility to record time-dependent processes. The scattering spectrum always is available and can be controlled directly by the user. The appearance of intense lines in the incident spectrum of a sealed tube, the energy dependence of

sample absorbance, and the detector response (see Sect. 1.3) make it difficult to interpret the spectrum quantitatively. For quantitative analysis one has to remove the $K\alpha$ and $K\beta$ lines from the *bremssstrahlung* spectrum as well as several fluorescence lines excited in the equipment by the incident photons. Therefore the energy-dispersive set-up is recommended for measurements on a relative scale, than for absolute measurements. However, using laboratory sources and choosing $\alpha_i \cong 1^\circ$, about 5 minutes sufficed to collect a spectrum of an organic multilayer sample with satisfying counting statistics [229].

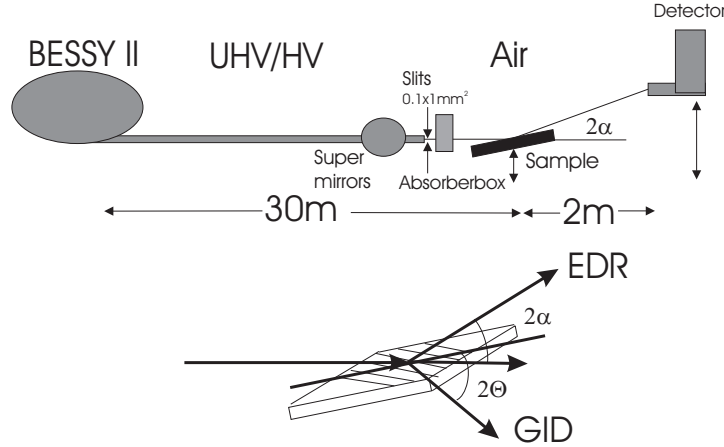


Fig. 2.3. Setup of the energy-dispersive reflectometer installed at the EDR beamline at BESSY II. It is equipped to measure simultaneously the reflectivity and grazing-incidence diffraction of a sample.

At the EDR beamline of BESSY II the same sample was measured in about 10 seconds with much better statistics [57]. Here energy-dispersive reflectometry is very efficient for rapid sample analysis and even for routine measurements.

Sample alignment is a crucial problem for accurate reflectivity measurements. In particular, the main error of density determination via measurement of the critical angle of total external reflection is the inaccurate sample alignment. Also a true specular scan can be recorded only when 2Θ is exactly twice ω . The procedure of alignment is same for an angle- and energy-dispersive set-up and will be explained in the following.

In order to measure the angles correctly, the rotational axis of the sample circle (ω -circle) has to be aligned exactly with the sample surface (Fig. 2.4). Additionally, one has to make sure that the position of the rotation axes of both circles coincides with the center of the incident beam; that means that the sample has to shadow half of the incident beam. With commercial

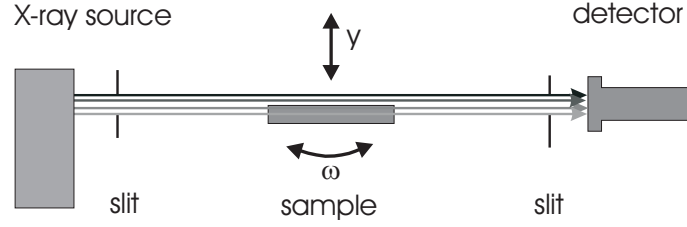


Fig. 2.4. Procedure to align the sample surface normal with the rotation axis of the reflectometer. This procedure is general for all types of reflectometers and diffractometers.

diffractometers it is a guarantee that the rotation axes of sample and detector coincide. However, the procedure to adjust the sample surface consists of an iterative movement and rocking of the sample across the incident beam (ω -scan). Both scans have to repeat until the peak intensity of the ω -scan is half of the intensity of the incident beam, measured without sample. In this case the ω -axis lies exactly in the sample surface and this surface is parallel to the incident-beam direction.

After this adjustment the angular position of the sample, however, may not coincide with the zero mark of the ω -circle. This might be caused by surface damage or by a miscut of the surface with respect to the bottom plane of the sample. Additional tests are necessary to redefine the ω -scale. To do this with sufficient accuracy one has to choose an incidence angle in the range $0 < \alpha_i < \alpha_c$ and find the angular position of specularly reflected beam at an angle 2θ . If 2θ does not coincide with $2\alpha_i$, the zero point of the ω -circle needs to be re-scaled by $(2\theta/2 - \alpha_i)$. Repetition of the procedure at various values of α_i improves the precision of sample alignment.

The reflectivity experiments should be optimized in such a way that the specular reflectivity can be measured over a wide range of α_i . This is necessary to show typical features as Bragg peaks and Kiessig fringes characterizing the sample. Due to the α^{-4} dependence of Fresnel reflectivity the intensity drops over 6 to 8 orders of magnitude. Sometimes it is helpful to record parts of a single reflectivity curve at different conditions of angular resolution and counting time. So the angular range close to α_c can be detected with the highest resolution available, but the wide angle range should be recorded using a relaxed resolution. Under home laboratory conditions one needs to change the angular resolution, i.e., to increase or decrease $\Delta\alpha_i$ and $\Delta\alpha_f$. When synchrotron radiation is used, separate detection of the low-angle and wide-angle range is necessary due to the limitation of detector sensitivity.

2.2 High-Resolution Diffractometer

In the semiconductor industry, in particular, the necessity to analyze epitaxially grown highly perfect multilayer materials encouraged the development of new types of diffractometers. They are well adapted to measure layer thickness, lattice mismatches and lattice strains of heterostructures. The investigation of quantum well structures, i.e., thin layers with thicknesses of less than 10 nm embedded within much thicker cladding layers, requires measurement of rocking curves over a wide angular range left and right with respect to the Bragg peak of the substrate. The method of reciprocal-space mapping makes it necessary to have good resolution in two directions of reciprocal space. All this requires a highly intense but parallel incident beam and a low background associated with a good as possible angular resolution. These needs should be satisfied by a high-resolution set-up at a synchrotron beamline. Unfortunately, due to the limited access, such experimental stations cannot be used for routine characterization. Thus, most of measurements have to be performed at home laboratories.

Modern high-resolution diffractometers are equipped with a four-bounce monochromator (Fig. 2.5). The intensity of the x-ray tube is increased by attaching a Göbel mirror. Maximum resolution, that is necessary for reciprocal-space mapping, is achieved by use of a channel-cut analyzer before the detector. As for reflectometers, the diffractometer makes motor-controlled angular steps $\Delta\omega = \Delta 2\theta \leq 0.001^\circ$ on both sample and detector circle. The equipment is suited to record reciprocal-space maps in the vicinity of a particular Bragg peak of the sample in several hours.

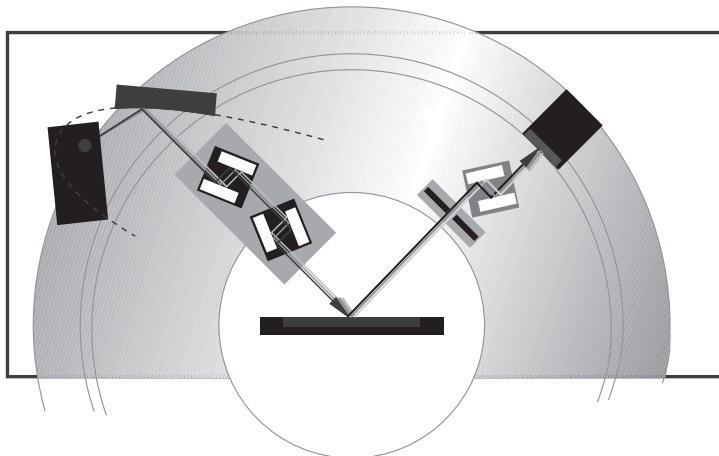


Fig. 2.5. High-resolution diffractometer.

The equipment shown in Fig. 2.5 should be simplified if the sample is not highly perfect. In this case the Bartels monochromator can be replaced by a single- or double-crystal arrangement. The analyzer crystal may be replaced by a slit system for simple rocking curve analysis. The achievable angular and energy resolution can be estimated using the DuMond diagrams shown in Sect. 1.2. Using $(+ -)$ set-up, the *dispersion enlargement* of each peak of the rocking curves follows from Eq. (1.10) identifying $\eta_{1,2}$ by the angular deviation from the diffraction maximum of the monochromator η_M and of sample η_S , respectively. The broadening of the diffraction curve can reach several hundred seconds of arc if the monochromator/analyzer and sample Bragg angles differ. In a strict sense, high resolution is achieved only if monochromator, sample, and analyzer are made from same material and scatter at exactly the same Bragg angles. The use of a four-bounce monochromator overcomes this problem. As demonstrated in Sect. 1.2, it combines the $+ -$ and $++$ set-up and allows one to measure always the intrinsic rocking curve of sample. Because the apparative broadening is very small, the the exploitable intensity is small compared with the usage of a double-crystal arrangement.

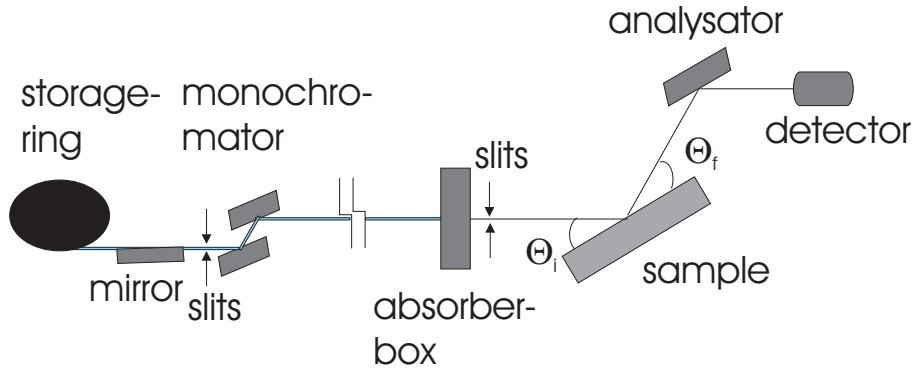


Fig. 2.6. General set-up of a high-resolution diffractometer equipped at a beamline of a storage ring facility.

All parts of the equipment have to be mechanically stable on a time scale of several hours or days so that reciprocal-space maps can be recorded under constant conditions (see Sect. 3.2). Reciprocal-space maps are obtained running ω -scans for different 2θ or running $(\omega + \omega_0) : 2\theta$ scans for different off-set angles ω_0 and plotting the recorded intensities in a 2D frame.

To run a particular scan across the reciprocal space, the sample and the detector circles have to move in an arbitrary ratio which differs from 1:2. These scans must be supported by the diffractometer software. In fact, computer software is an essential component of modern diffractometers. Fast

access to a code of rocking curve simulation enables interpretation of the experimental curves straight after the measurement and interactive action. However, the user has to make sure beforehand that the basic assumptions of the simulation software agrees with those of the actual experiment.

Finally we propose an optimum arrangement for high-resolution diffraction which can be installed at a beamline at a synchrotron radiation facility. A schematic set-up is shown in fig. 2.6. Because the demand for intensity is not as high (about 8 orders of magnitude are sufficient) the high photon flux delivered by an undulator can be used to design a setup with very good angular resolution. A heavyweight goniometer can help to guarantee reproducible steps of less than 0.0005° . The small divergence of the synchrotron radiation in vertical direction should not be enlarged by bent mirrors. Plane monochromator crystals performed by a double-crystal arrangement supply an energy band pass with a resolution on the order of 10^{-4} . A collimation line defined by two pairs of slits, a guiding slit pair straight after the monochromator and a defining slit pair close before the sample, reduce the divergence of the incident beam. Supposing a source height of $100\text{ }\mu\text{m}$ and a length of the beamline of 20 m, the slit height of 1 mm provides a divergence of less than one second of arc, which is much smaller than the intrinsic half-width of the silicon monochromator crystal (see Fig. 1.5). Despite these constraints the flux at the sample site will exceed 10^{12} photons/sec if we choose a typical undulator beamline of ESRF. Finally a plane monochromator should be attached close before the point detector to guarantee high-resolution of the exit angle α_f , as well.

2.3 Limits of the Use of Powder Diffractometers

Several problems of x-ray characterization can be solved by using low-resolution diffractometers, i.e., a powder diffractometer. If the layered material is damaged, the Bragg peaks become broad and low in intensity. Following Eq. (1.8), the divergence of the incident beam should not be much smaller than the angular width of the diffraction curve of the sample under investigation. In the case of poly-crystalline material or material with a mosaic spread the intrinsic curve width may increase to several minutes of arc. Here focusing beam arrangements are preferred. A bent crystal-monochromator or analyzer in front of the sample or the detector, respectively, provides increased intensity and a relaxed angular resolution. A disadvantage of this arrangement is the simultaneous appearance of the $K\alpha$ doublet in the rocking curve, which has to be taken into account for the simulation of the diffraction curves.

Figure 2.7 shows the (422) diffraction curves of a partially relaxed 40 period $\text{In}_{0.2}\text{Ga}_{0.8}\text{As}/\text{GaAs}$ multilayer recorded, first, with a graphite-analyzer-equipped powder diffractometer, similar to that shown in Fig. 2.2 and, second, under high-resolution conditions (see Fig. 2.5) using a four-bounce monochromator without Göbel mirror. The time taken to record the high-resolution

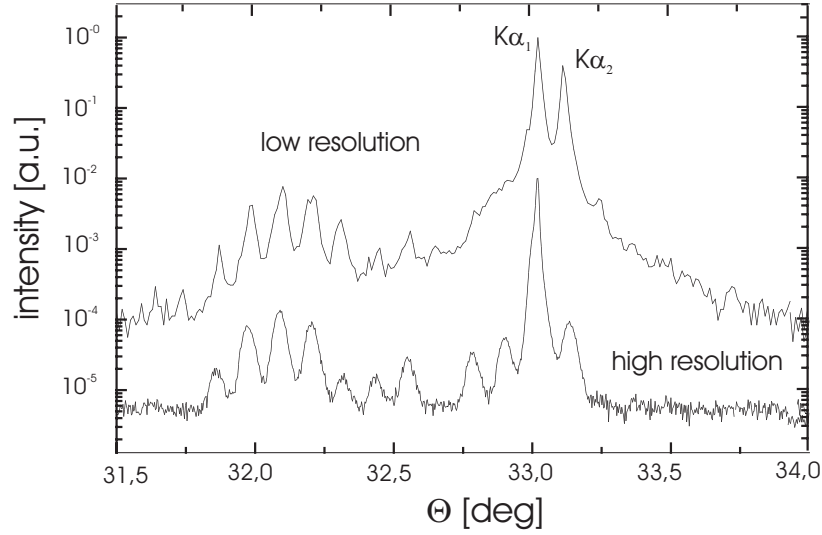


Fig. 2.7. Rocking curve of an $\text{In}_{0.2}\text{Ga}_{0.8}\text{As}/\text{GaAs}$ multilayer recorded with a powder diffractometer, similar to that shown in Fig. 2.2, and with high-resolution conditions, using a four-bounce monochromator.

curve was about five times longer than that for the powder diffractometer. The main difference between both curves is the appearance of the $K\alpha_2$ line at the powder curve. Except in the region close to the substrate peak, the superlattice peaks are clearly visible. Here, they are smeared out because of the lower angular resolution compared with the high-resolution curve. Because the measured angular width of superlattice peaks is determined by the mosaicity, the structure parameters of the multilayer sample can be estimated on the basis of this powder curve [290].

2.4 Grazing-Incidence Diffraction

A schematic illustration of the set-up of a grazing-incidence diffraction (GID) experiment is shown in Fig. 2.8 [89, 281]. Here one has to distinguish between the *plane of incidence* containing α_i and α_f and the surface normal and the *scattering plane* lying approximately perpendicular to the plane of incidence and containing the angles θ_i and θ_f . The latter ones are measured with respect to the diffracting lattice plane. The method unifies in-plane Bragg diffraction and out-of-plane reflectivity combined with the feasibility for depth resolution.

The experimental set-up is the following: a monochromatic and parallel x-ray beam as defined in Fig. 2.6 strikes the sample surface at an angle α_i close

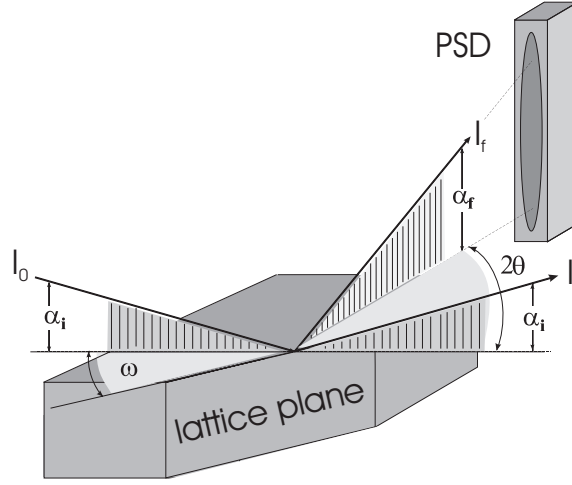


Fig. 2.8. Schematic set-up of a grazing-incidence diffraction experiment.

to the critical angle α_c . The sample is rotated around the surface normally until a particular lattice plane lying perpendicular to the surface fulfills the Bragg condition under an in-plane Bragg angle $2\theta_{B||} = \theta_i + \theta_f$ (see Sect. 3.3).

Owing to refraction of the incoming beam at the air-sample interface the penetration depth of the probing x-ray can be controlled by choosing α_i to be smaller or larger than α_c (Fig. 2.9). In the first case the incoming beam becomes evanescent and propagates parallel to and close below the surface. The minimum penetration depth is on the order of 4–10 nm, depending on the density of material. On increasing α_i , the penetration depth within the sample increases up to about 400–600 nm.

The GID geometry requires collimation in both directions, perpendicular and parallel to the plane of incidence. In general, a set-up like that shown in Fig. 2.6 can be used but with additional efforts to gain the in-plane resolution. In fact, one needs a second monochromator installed perpendicular to the first one; this reduces the photon flux at the sample site again. For practical reasons the divergence with respect to α_i should be one order of magnitude smaller than that with respect to $2\theta_{B||}$. On the other hand, a moderate divergence regarding $2\theta_{B||}$ is necessary to excite the crystal truncation rod (CTR) (see Sect. 3.2). The intensity distribution along the crystal truncation rod can be recorded simultaneously as a function of α_f using a position-sensitive detector (Sect. 1.3). The measurement of reciprocal-space maps requires the insertion of an analyzer crystal. Because the reflectivity of the truncation rod is on the order of 10^{-8} , the intensity of a sealed tube is not enough to record in-plane scattering curves. The intensity of a rotational-

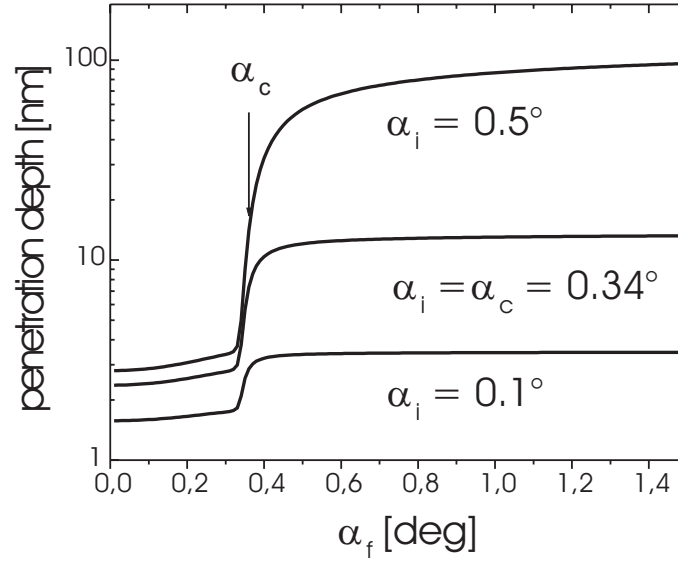


Fig. 2.9. The effective penetration depth below a GaAs surface for a GID experiment, calculated for different incidence angles α_i and exit angle α_f .

anode is sufficient for the detection of in-plane rocking curves integrated over the whole α_f range, i.e., with a wide open detector window. The measurement of α_f -resolved curves with good angular resolution is only possible with use of synchrotron radiation. α_f integrated measurement can also be performed using the energy-dispersive arrangement shown in Fig. 2.3.

High-Resolution X-Ray Scattering
From Thin Films to Lateral Nanostructures
Pietsch, U.; Holy, V.; Baumbach, T.
2004, XVI, 408 p. 389 illus., Hardcover
ISBN: 978-0-387-40092-1